




Article

B-10-Based Macrostructured Cathode for Neutron Detectors

Alexander G. Kolesnikov ^{1,2,*}, Aleksey K. Kurilkin ¹ , Viktor I. Bodnarchuk ^{1,2,3} , Alexander S. Ovodov ¹
and Marat R. Gafurov ⁴ 

¹ Frank Laboratory of Neutron Physics, Joint Institute for Nuclear Research, 6 Joliot-Curie St., Dubna 141980, Russia; akurilkin@jinr.ru (A.K.K.); bodnarch@nf.jinr.ru (V.I.B.)

² Dubna State University, 19 Universitetskaya St., Dubna 141980, Russia

³ National Research Centre “Kurchatov Institute”, 1 Academician Kurchatov Sq., Moscow 123182, Russia

⁴ Institute of Physics, Kazan Federal University, 18 Kremlevskaya St., Kazan 420008, Russia

* Correspondence: agkol@jinr.ru

Abstract: This paper focuses on the search for the desired thickness of the $^{10}\text{B}_4\text{C}$ thin-film coating, as well as the macrostructuring of the aluminum foil substrate used as a cathode in the production of a multiwire gas detector of thermal neutrons. The impact of the $^{10}\text{B}_4\text{C}$ film thickness from 1.0 to 2.5 μm and of the 0.05 mm thick Λ -shaped macrostructured aluminum foil substrate with an angle at the Λ -vertex from 10 to 45 degrees, with a height from 0.5 to 4 mm and a distance between the Λ -structures from 0.1 to 0.8 relative units on the neutron registration efficiency 1.8\AA , was investigated. Numerical modeling of the electrostatic field was carried out using the Elcut software package. The interaction of neutrons with the $^{10}\text{B}_4\text{C}$ thin-film coating was modeled using the Monte Carlo method in the Geant4 program. The optimal values of the geometrical parameters for the best neutron registration efficiency were determined.

Keywords: neutron detector; ^{10}B converter; macrostructured cathode



Academic Editor: Milan Tichý

Received: 7 December 2024

Revised: 14 January 2025

Accepted: 29 January 2025

Published: 2 February 2025

Citation: Kolesnikov, A.G.; Kurilkin, A.K.; Bodnarchuk, V.I.; Ovodov, A.S.; Gafurov, M.R. B-10-Based Macrostructured Cathode for Neutron Detectors. *Coatings* **2025**, *15*, 168. <https://doi.org/10.3390/coatings15020168>

Copyright: © 2025 by the authors. Licensee MDPI, Basel, Switzerland. This article is an open access article distributed under the terms and conditions of the Creative Commons Attribution (CC BY) license (<https://creativecommons.org/licenses/by/4.0/>).

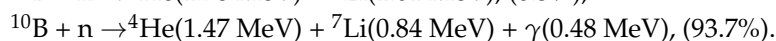
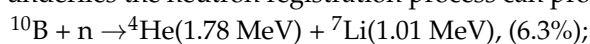
1. Introduction

The pursuit of optimal solutions in the design of detector systems for the registration of thermal neutrons represents a critical challenge in the advancement of neutron scattering facilities. The effectiveness of any such facility is fundamentally linked to the sophistication of its detector system. Given that neutrons do not directly ionize the gaseous medium, it is essential to employ a conversion material that transforms neutron radiation into charged particles. One of the most effective charge converters available is gaseous helium-3 (^3He). This isotope has a high thermal neutron capture cross-section ($\sigma = 5328$ barn for neutron energy $E_n = 0.025$ eV). The underlying mechanism involves the following capture reaction [1]: $^3\text{He} + n \rightarrow p (0.57 \text{ MeV}) + ^3\text{H} (0.19 \text{ MeV})$. In this context, the converter serves a dual purpose, functioning both as the conversion medium and the working gas. This dual functionality contributes significantly to the widespread use of ^3He -based detection systems [1].

In certain instances, ^3He detectors may not fully exploit the capabilities of the neutron facilities. Key drawbacks of ^3He detectors include not only the substantial expense associated with the ^3He isotope but also the requirement for elevated gas pressure within the detector chamber. This necessity results in an increased thickness of the detector's entrance window. Such an increase restricts the detector's capacity to detect neutrons in the colder regions of the energy spectrum, as the absorption and scattering cross-sections in the wall material significantly rise for these neutrons, consequently diminishing the quality of the experimental data. Furthermore, the dual function of ^3He gas as both a converter and a

working gas constrains the detector's maximum loading capacity (approximately 1 MHz) and spatial resolution (at least 1 mm) [2]. For many applications, these specifications are adequate, ensuring a continued demand for ^3He converters. Nevertheless, when there is a necessity to surpass these constraints, it becomes essential to investigate alternative approaches for neutron detection.

The isotope ^{10}B is frequently regarded as a viable substitute. The neutron capture cross-section of isotope ^{10}B ($\sigma = 3837$ barn, $E_n = 0.025$ eV) is approximately 28% less than that of ^3He . The natural abundance of this isotope is about 20%, and it is feasible to enrich its content up to 95%, with a purity degree of 99.9%. The application of isotope ^{10}B as a neutron radiation converter can be realized through the solid boron carbide compound B_4C , which possesses a stable structure and a density of 2.52 g/cm³. The nuclear reaction that underlies the neutron registration process can proceed in two ways [1]:



The reaction is characterized by a substantial release of energy. Due to the relatively low energy of thermal neutrons in comparison to the energy of the emitted particles, the ^7Li nucleus and the α -particle fly isotropically in opposite directions. Since boron carbide is a dense solid, this allows for better localization in determining the neutron capture site, which helps to significantly improve the spatial resolution of detectors (see, e.g., [3]). However, the high density of the material restricts the free escape of charged particles that are products of the reaction from the converter medium. Consequently, it becomes necessary to utilize a $^{10}\text{B}_4\text{C}$ converter in the form of a thin-film coating, typically a few micrometers in thickness. This requirement, however, results in reduced registration efficiency. Several strategies exist to enhance efficiency under these conditions. One is to increase the number of layers in the neutron beam path, another is to orient the $^{10}\text{B}_4\text{C}$ layer at a small angle to increase the effective path length in the converter material without increasing its thickness, a technique referred to as inclined geometry. Both strategies have been implemented to varying extents in operational detectors, yielding satisfactory results. This evidence suggests that detectors utilizing a $^{10}\text{B}_4\text{C}$ converter can achieve registration efficiencies comparable to those of ^3He detectors [4,5].

In this study, we explore an alternative method for the implementation of neutron detectors utilizing a $^{10}\text{B}_4\text{C}$ converter, aiming to significantly enhance detection efficiency. The proposed approach involves structuring the cathode plane of the detector into sharp ridges, which are coated with a thin layer of B_4C , as illustrated in Figure 1. This concept effectively embodies the principle of inclined geometry, positioning the boron carbide layer at a slight angle relative to neutron radiation, achieved through the structuring of the cathode surface. While this concept is not entirely novel, as evidenced in references [6,7], it has been shown that a structured cathode can be an effective means of improving the resolving power or efficiency of the detector. In this paper, we advance this methodology and demonstrate through modeling that specific geometric configurations of this system can yield high neutron detection efficiency.

Schematic view of a macrostructured cathode

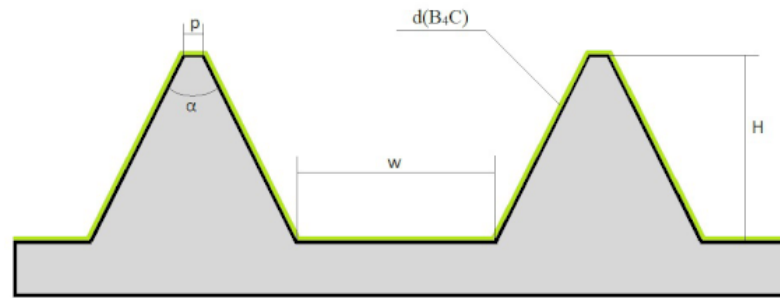


Figure 1. Schematic view of macrostructured cathode.

2. Modeling of Single-Layer Detector with Macrostructured Cathode

Modeling of the detector efficiency with a macrostructured cathode was performed using the Geant4 software package version 10.07.p02 [8] and the program for engineering simulation of electrostatic fields by the finite element method ELCUT [9]. The macrostructured cathode is a Λ -shaped surface, the schematic representation of which is shown in Figure 1. The Λ -shaped form is characterized by the angle α at the top, the height H of the macrostructure, the thickness d of the $^{10}\text{B}_4\text{C}$ neutron converter coating, and the width of the window W .

Aluminum is chosen as the cathode material, with a uniformly deposited layer of $^{10}\text{B}_4\text{C}$. The detector neutron registration efficiency is calculated for a neutron beam with $\lambda = 1.8 \text{ \AA}$. The beam used in the simulation is a quantized flux of 10^8 neutrons incident perpendicular to the cathode surface and uniformly distributed over the detector area of 10 mm width and 40 mm length. A mixture of $\text{CF}_4/\text{C}_4\text{H}_{10}$ (80/20%) was chosen as the working gas. The density of the $^{10}\text{B}_4\text{C}$ coating layer and the degree of enrichment of the converter with ^{10}B isotope were calculated to be 2.2 g/cm^3 and 95%, respectively. The detector efficiency is defined as the ratio of the number of secondary particles of the reaction $^{10}\text{B}(n,^4\text{He})^7\text{Li}^*$, ^7Li flying out into the gas to the number of neutrons and is calculated taking into account the depth of penetration of the electrostatic field into the macrostructure, as well as taking into account the threshold on the energy left by ^4He and ^7Li particles in the $\text{CF}_4/\text{C}_4\text{H}_{10}$ gas mixture. The examination of the electrostatic field is crucial, particularly when the window width W is minimal, as the field exhibits limited penetration into the macrostructure. Consequently, electrons generated from gas ionization by ^4He and ^7Li particles within regions characterized by a weak electrostatic field, situated at a certain depth from the macrostructure's surface, will not be directed towards the anode. This lack of electron extraction results in an absence of neutron registration signals, ultimately diminishing the efficiency of the detector. Figure 2 illustrates the outcomes of electrostatic field modeling conducted with the ELCUT program for $H = 2 \text{ mm}$. To account for the effects of field penetration depth, an approximation was employed whereby the efficiency values derived from Geant4 were normalized using the factor $(1-h/H)$, with H representing the height defined by the static voltage threshold at the center of the window W . The threshold value was set at $U = 1 \text{ V}$.

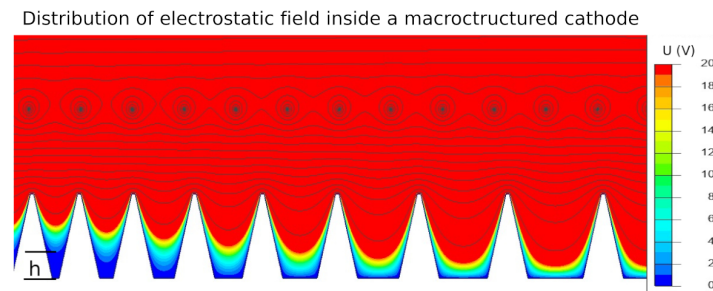


Figure 2. Electrostatic field distribution inside detector with macrostructured cathode at $H = 2$ mm.

3. Results of Calculations of Efficiency of a Single-Layer Detector with a Macrostructured Cathode

Modeling of the efficiency of a single-layer detector with a macrostructured cathode was performed for angles $\alpha = 10^\circ, 15^\circ, 20^\circ, 30^\circ, 45^\circ$; for heights H from 0.5 to 4 mm in steps of 0.5 mm; for layer thicknesses $^{10}\text{B}_4\text{C}$ from 1.0 to 2.5 μm in steps of 0.5 μm ; and for window widths defined by the expression $W = H \times i$, where i represents the window width in relative units increasing from 0.1 to 0.8 in steps of 0.1. The value i is introduced to perform scaling of macrostructured cathodes for different heights H .

The calculated efficiency of a single-layer detector with a macrostructured cathode covered with a 1000 nm thick layer of $^{10}\text{B}_4\text{C}$ as a function of the window width in relative units (i) at different heights H for angles $\alpha = 10^\circ$ and 30° is shown in Figure 3. The calculations indicate that for $H \geq 1$ mm, there is an optimal value of i for each angle α , where the efficiency reaches its maximum. In contrast, for $H < 1$ mm (approximately at $H = 0.5$ mm), the efficiency reaches a plateau and practically does not decrease with increasing window width. The optimal window width values in relative units, which yield efficiencies nearing their maximum for most heights of the macrostructure, are identified as follows: 0.4 for $\alpha = 10^\circ$ and 15° ; 0.3 for $\alpha = 20^\circ$ and 30° ; and 0.2 for $\alpha = 45^\circ$. The subsequent analyses of neutron registration efficiency will be conducted using these window width parameters.

In order to further characterize macrostructured cathodes coated with $^{10}\text{B}_4\text{C}$, we introduced a neutron utilization factor. This factor is defined as the ratio of the number of neutrons detected by a single-layer detector to the number of reactions ($n+^{10}\text{B}$) resulting from neutron interactions with the ^{10}B converter. This approach is analogous to the utilization factor used for magnetron target materials. The relationship of this factor with respect to the height H at angles $\alpha = 10^\circ$ and 15° , 0.3 for $\alpha = 20^\circ$ and 30° , and 0.2 for $\alpha = 45^\circ$ is illustrated for various thicknesses of the $^{10}\text{B}_4\text{C}$ layer ($d = 1000$ nm, 1500 nm, 2000 nm, and 2500 nm), both with and without an energy threshold, as depicted in Figures 4–7. Additionally, the efficiency of neutron registration as a function of H is shown. The dashed lines represent the efficiency of a single-layer detector with a flat cathode corresponding to the specified coating thicknesses. The energy thresholds for the particles ^4He and ^7Li in the gas are set at 0 and 120 keV, respectively. At the 0 keV threshold, the graphs indicate the maximum potential values, considering the influence of an electrostatic field at a level of 1 V. Conversely, at the 120 keV threshold, the graphs reflect more realistic values that can be experimentally achieved. The choice of threshold energy 120 keV to n- γ discrimination is based on the study of response of the detector to the γ -field emitting by a neutron source ^{252}Cf [10].

Detector efficiency at different window width

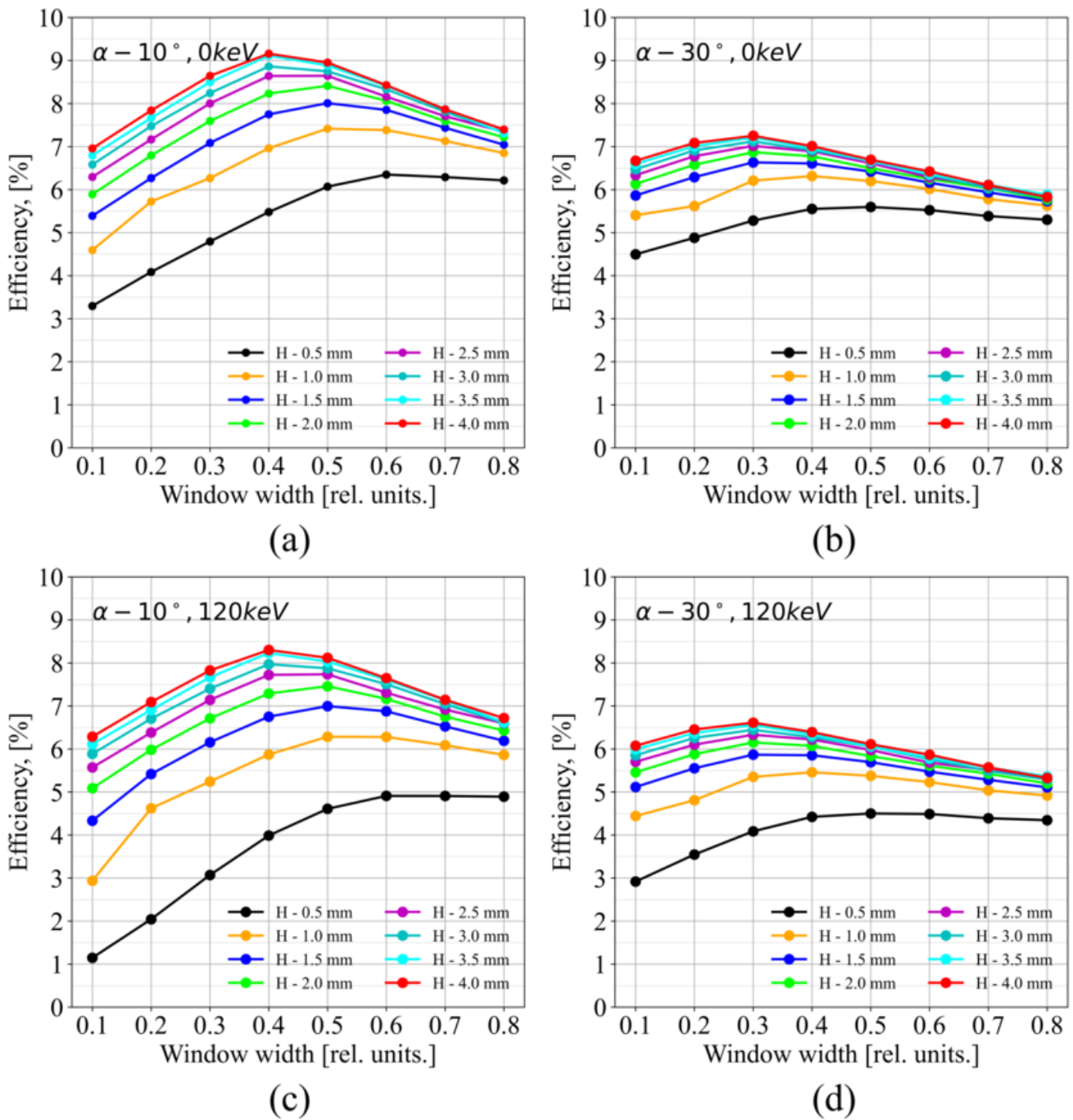


Figure 3. (a) Efficiency of detector at $\alpha 10^\circ$ and threshold 0 keV. (b) Efficiency of detector at $\alpha 30^\circ$ and threshold 0 keV. (c) Efficiency of detector at $\alpha 10^\circ$ and threshold 120 keV. (d) Efficiency of detector at $\alpha 30^\circ$ and threshold 120 keV.

Within the context of the selected model, and considering the penetration of the electrostatic field into the macrostructure, the computational results indicate that the efficiency of a single-layer detector featuring a macrostructured cathode improves as the height H increases, ultimately reaching a plateau at approximately 3–4 mm. For $H \leq 1$ mm, the efficiency differences for angles $\alpha = 10^\circ, 15^\circ, 20^\circ$ and 30° are minimal. Conversely, for heights $H \geq 1$ mm, the efficiencies for cathodes at angles $\alpha = 10^\circ$ and 15° exhibit

similar and optimal efficiency values among the various combinations of α , H , and W . The efficiency of the detector with a macrostructured cathode at an angle of $\alpha = 20^\circ$ is slightly lower than that of angles $\alpha = 10^\circ$ and 15° , yet it is more feasible to manufacture. It is important to highlight that employing a macrostructured cathode, as opposed to a flat cathode, can enhance efficiency by approximately 2–3 times, achieving peak values around 10%–11% for a $^{10}\text{B}_4\text{C}$ layer thickness of 2500 nm.

However, it should be noted that an increase in the thickness of the $^{10}\text{B}_4\text{C}$ layer leads to a decline in the neutron utilization factor. Specifically, for a $^{10}\text{B}_4\text{C}$ layer thickness exceeding 2000 nm and a threshold of 120 keV, the neutron utilization factor falls below 50%. In contrast, for a $^{10}\text{B}_4\text{C}$ layer thickness of 1000 nm at heights greater than 2 mm, the neutron utilization factor can reach approximately 60%–70%. A reduction in detector efficiency of about 3% corresponds to an increase in the neutron utilization factor by more than 10%–20%. These findings suggest that to optimize efficiency in the design of multilayer detectors with a structured cathode, it is essential to consider not only the efficiency of a single-layer detector but also the neutron utilization factor.

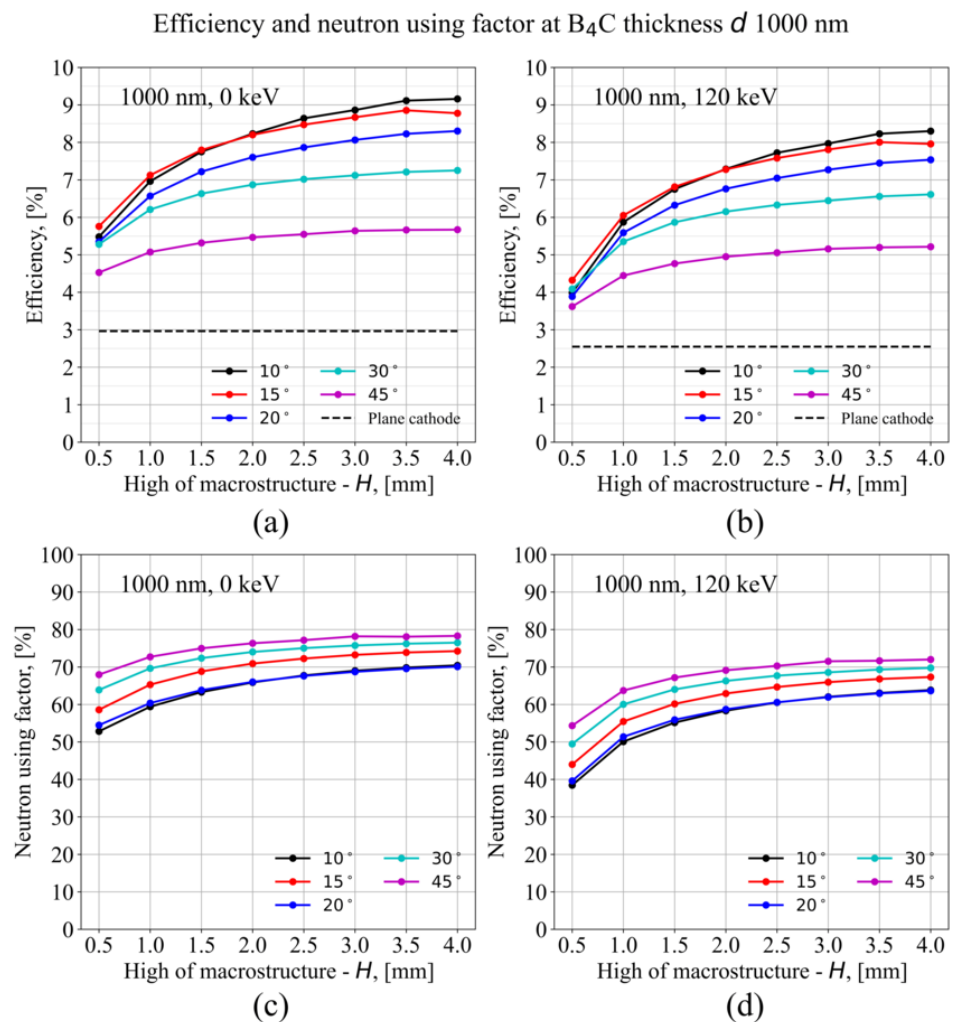


Figure 4. (a) Efficiency of detector at $d(\text{B}_4\text{C}) = 1000$ nm and threshold 0 keV. (b) Efficiency of detector at $d(\text{B}_4\text{C}) = 1000$ nm and threshold 120 keV. (c) Neutron using factor at $d(\text{B}_4\text{C}) = 1000$ nm and threshold 0 keV. (d) Neutron using factor at $d(\text{B}_4\text{C}) = 1000$ nm and threshold 120 keV.

Efficiency and neutron using factor at B₄C thickness d 1500 nm

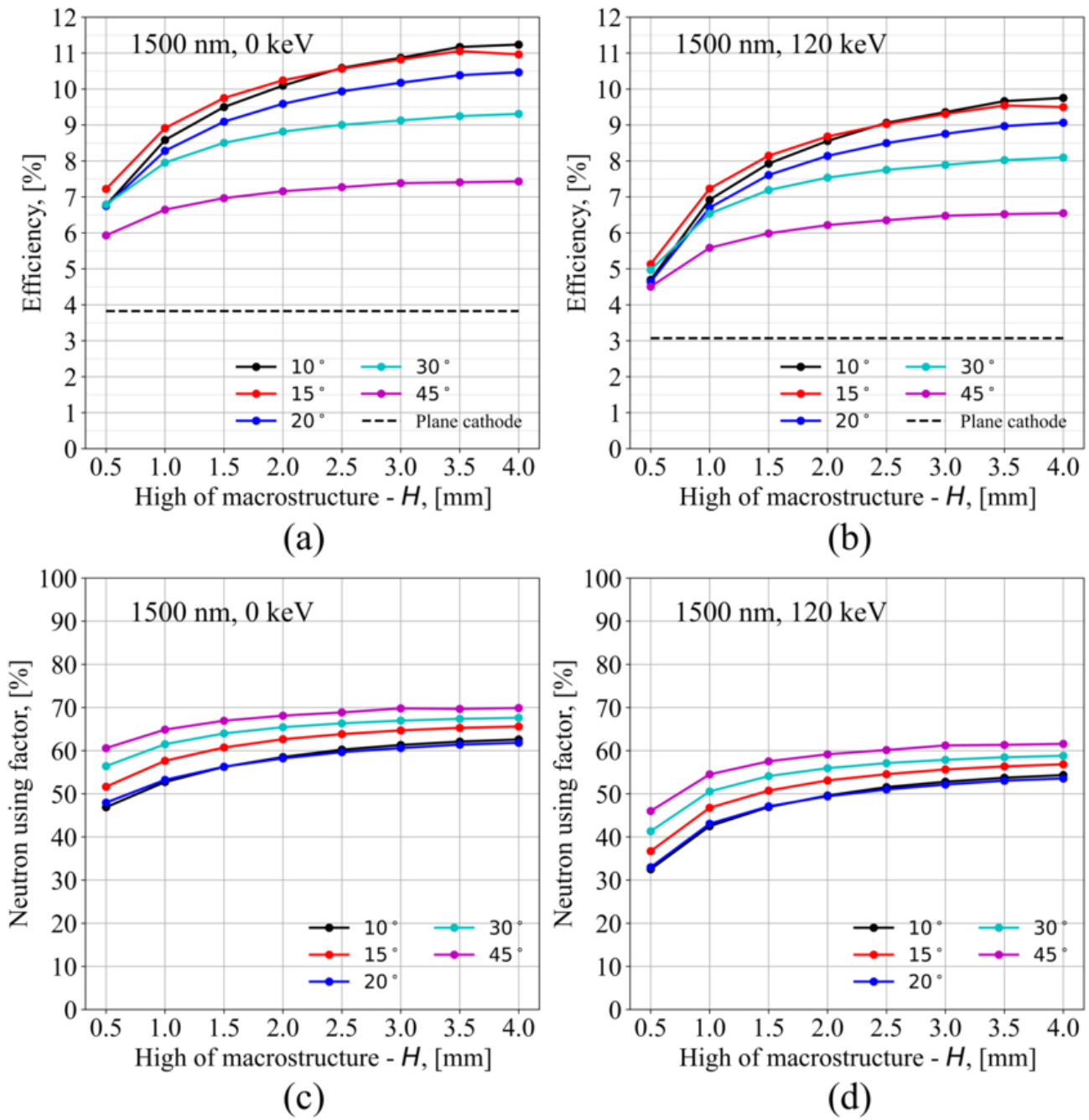


Figure 5. (a) Efficiency of detector at $d(\text{B}_4\text{C}) = 1500$ nm and threshold 0 keV. (b) Efficiency of detector at $d(\text{B}_4\text{C}) = 1500$ nm and threshold 120 keV. (c) Neutron using factor at $d(\text{B}_4\text{C}) = 1500$ nm and threshold 0 keV. (d) Neutron using factor at $d(\text{B}_4\text{C}) = 1500$ nm and threshold 120 keV.

Efficiency and neutron using factor at B₄C thickness *d* 2000 nm

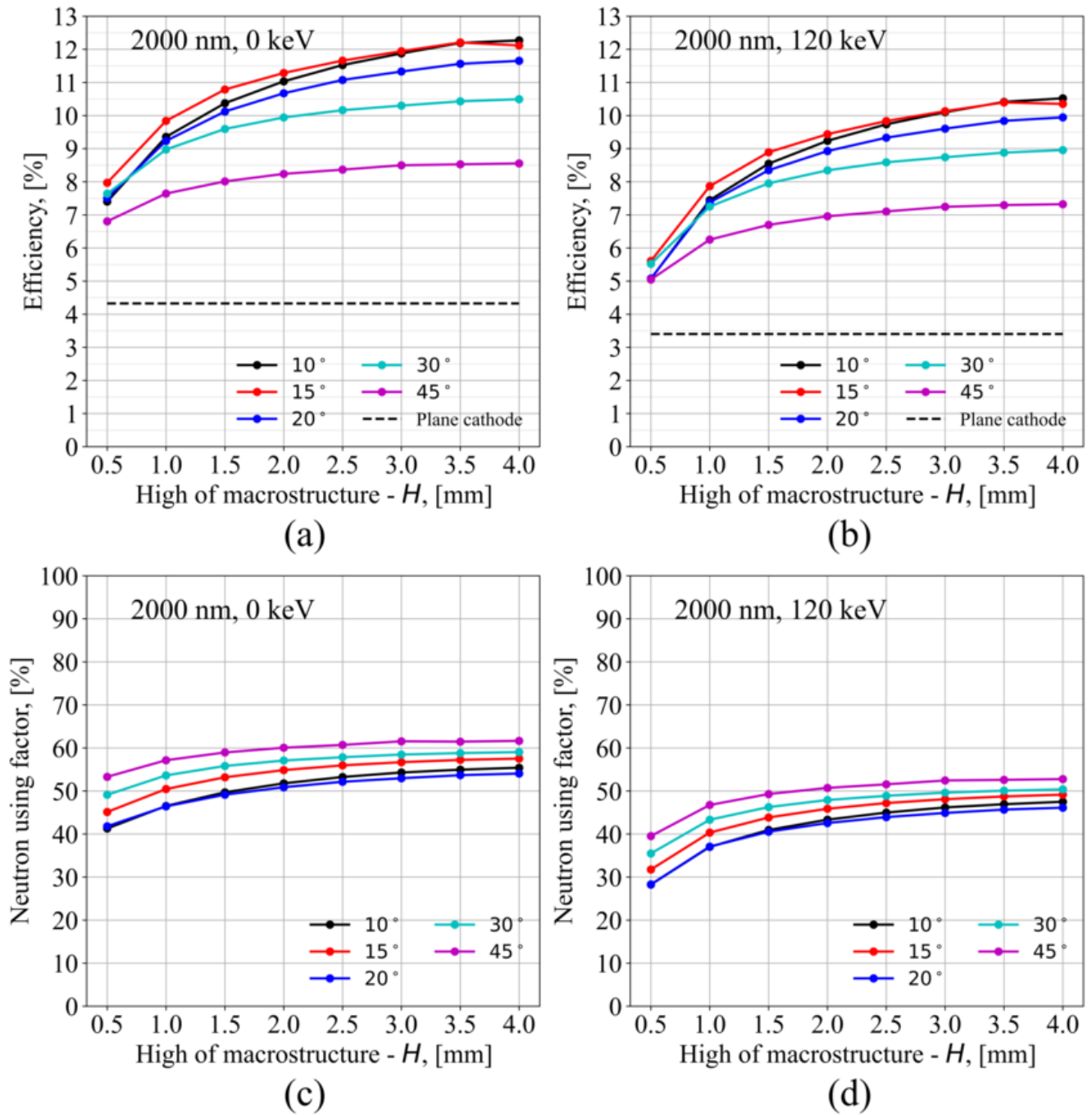


Figure 6. (a) Efficiency of detector at $d(B_4C) = 2000$ nm and threshold 0 keV. (b) Efficiency of detector at $d(B_4C) = 2000$ nm and threshold 120 keV. (c) Neutron using factor at $d(B_4C) = 2000$ nm and threshold 0 keV. (d) Neutron using factor at $d(B_4C) = 2000$ nm and threshold 120 keV.

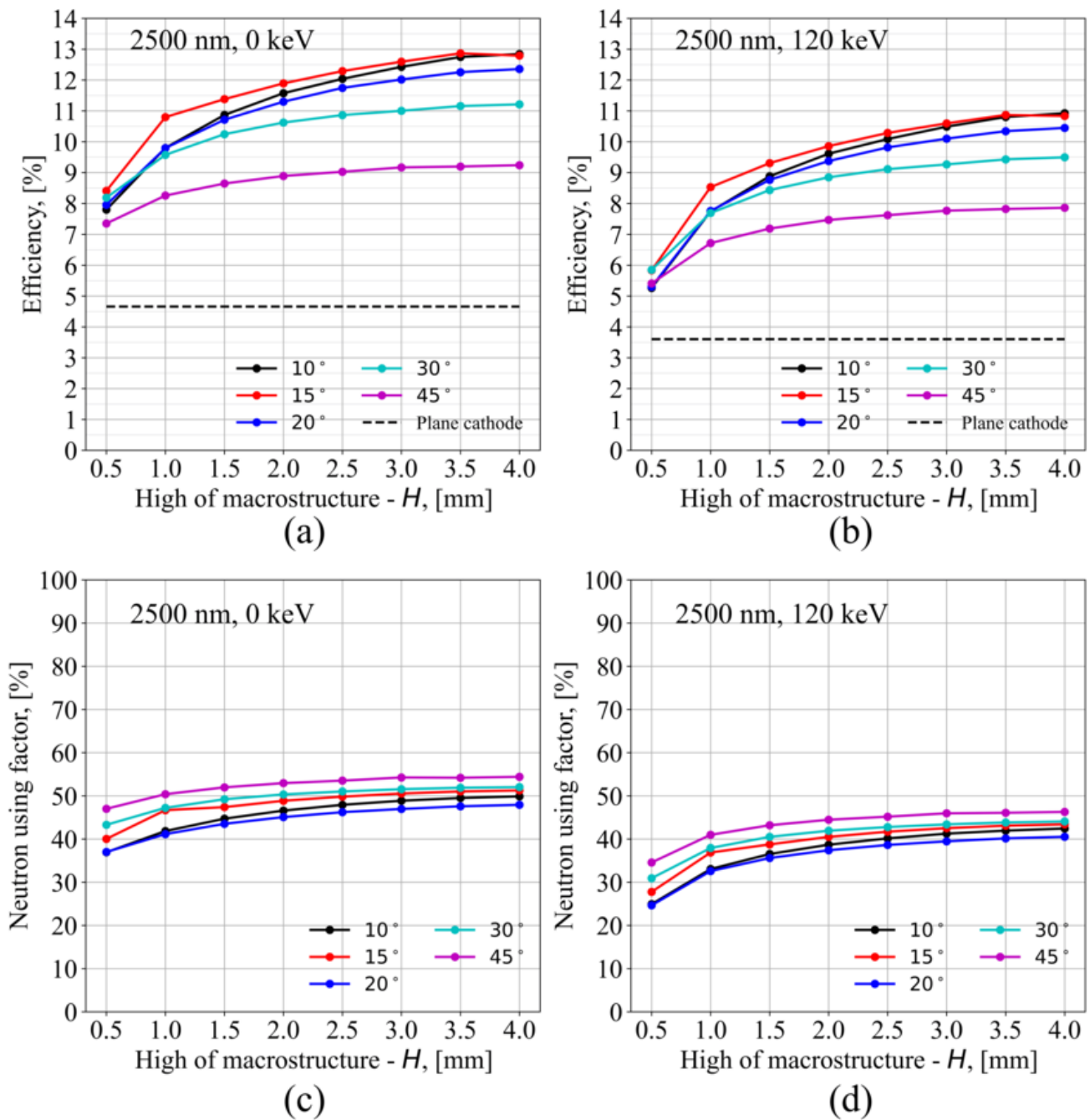
Efficiency and neutron using factor at B_4C thickness d 2500 nm

Figure 7. (a) Efficiency of detector at $d(B_4C) = 2500$ nm and threshold 0 keV. (b) Efficiency of detector at $d(B_4C) = 2500$ nm and threshold 120 keV. (c) Neutron using factor at $d(B_4C) = 2500$ nm and threshold 0 keV. (d) Neutron using factor at $d(B_4C) = 2500$ nm and threshold 120 keV.

4. Conclusions

This study presents the potential for developing neutron detectors featuring a macrostructured cathode. Modeling results of single-layer detectors incorporating this type of cathode, while considering the influence of the electrostatic field on the macrostructure, indicate an enhancement in detection efficiency by a factor of two to three when compared to traditional single-layer detectors equipped with a flat cathode. The optimal efficiency achievable for a single-layer detector utilizing a macrostructured cathode is approximately

10%–11% at a sputtering thickness of 2500 nm, with an energy threshold set at 120 keV. Various geometric configurations of this system are capable of achieving elevated neutron detection efficiency.

Author Contributions: Methodology, A.G.K.; Validation, V.I.B.; Formal analysis, A.K.K.; Investigation, A.S.O.; Resources, V.I.B.; Writing—original draft, M.R.G. All authors have read and agreed to the published version of the manuscript.

Funding: This research was funded by the Ministry of Science and Higher Education of the Russian Federation (Agreement No. 075-10-2021-115 from 13 October 2021 (internal number 15.SIN.21.0021).

Institutional Review Board Statement: Not applicable.

Informed Consent Statement: Not applicable.

Data Availability Statement: Data are contained within the article.

Conflicts of Interest: The authors declare no conflicts of interest.

References

1. Henzlova, D.C.; Baker, M.P.; Bartlett, K.; Favalli, A.; Iliev, M.; Root, M.A.; Sarnoski, S.; Shin, T.; Swinhoe, M.T. Neutron Detectors. In *Nondestructive Assay of Nuclear Materials for Safeguards and Security*; Geist, W.H., Santi, P.A., Swinhoe, M.T., Eds.; Springer: Cham, Switzerland, 2024. [CrossRef]
2. Guerard, B.; Hall-Wilton, R.; Murtas, F. Prospects in MPGDs development for neutron detection. *arXiv* **2014**, arXiv:1410.0107. [CrossRef]
3. Margato, L.M.S.; Morozov, A.; Blanco, A.; Fonte, P.; Lopes, L.; Zeitelhack, K.; Hall-Wilton, R.; Höglund, C.; Robinson, L.; Schmidt, S.; et al. Multilayer ^{10}B -RPC neutron imaging detector. *J. Instrum.* **2020**, *15*, P06007. [CrossRef]
4. Anastasopoulos, M.; Bebb, R.; Berry, K.; Birch, J.; Bryś, T.; Buffet, J.C.; Clergeau, J.F.; Deen, P.P.; Ehlers, G.; Van Esch, P.; et al. Multi-Grid detector for neutron spectroscopy: Results obtained on time-of-flight spectrometer CNCS. *J. Instrum.* **2017**, *12*, P04030. [CrossRef]
5. Messi, F.; Mauri, G.; Piscitelli, F. The Milti-Blade: The ^{10}B -based neutron detector for reflectometry at ESS. *Nucl. Inst. Methods Phys. Res. A* **2019**, *936*, 499–500. [CrossRef]
6. Fujiwara, T.; Takahashi, H.; Yamada, N.L.; Uesaka, M. Microstructure Boron detector for high efficiency thermal neutron detection. In Proceedings of the 2013 IEEE Nuclear Science Symposium and Medical Imaging Conference, Seoul, Republic of Korea, 27 October–2 November 2013. [CrossRef]
7. Stefanescu, I.; Abdullahi, Y.; Birch, J.; Defendi, I.; Hall-Wilton, R.; Höglund, C.; Hultman, L.; Zee, M.; Zeitelhack, K. A ^{10}B -based neutron detector with stacked MultiWire Proportional Counters and macrostructured cathodes. *J. Instrum.* **2013**, *8*, P12003. [CrossRef]
8. Agostinelli, S.; Allison, J.; Amako, K.A.; Apostolakis, J.; Araujo, H.; Arce, P.; Asai, M.; Axen, D.; Banerjee, S.; Barr, G.J.N.I.; et al. GEANT4—A simulation toolkit. *Nucl. Instrum. Meth. A* **2003**, *506*, 250. [CrossRef]
9. Available online: <https://elcut.ru/> (accessed on 7 December 2024).
10. Stefanescu, I.; Abdullahi, Y.; Birch, J.; Defendi, I.; Hall-Wilton, R.; Höglund, C.; Hultman, L.; Seiler, D.; Zeitelhack, K. Development of a novel macrostructured cathode for large-area neutron detectors based on the ^{10}B -containing solid converter. *Nucl. Inst. Meth. A* **2013**, *727*, 109. [CrossRef]

Disclaimer/Publisher's Note: The statements, opinions and data contained in all publications are solely those of the individual author(s) and contributor(s) and not of MDPI and/or the editor(s). MDPI and/or the editor(s) disclaim responsibility for any injury to people or property resulting from any ideas, methods, instructions or products referred to in the content.